Unguided crack growth simulation in asymmetric specimens using bond-based peridynamics

Asghar Sami[1] and Umit Keskin[2]

[1]*Graduate Student, Islamic Azad University, Tabriz Branch, Tabriz, Iran*
[2]*Graduate Student, Okan University, Istanbul, Turkey*

Abstract – *Peridynamics is a nonlocal continuum theory which reformulates the classical mechanics by substituting the differential term with integral term. Therefore, the peridynamic formulation is valid everywhere regardless of presence of discontinuities such as cracks. This makes peridynamics a robust and promising technique in predicting failure in engineering materials and structures. This work aims to develop peridynamic simulations to model unguided crack growth in asymmetric specimens. The presence of asymmetric circular notches around a macro crack tip has been studied on damage pattern of a pre-cracked specimen. The results indicates that peridynamics is successfully able to simulate complex failure modes in engineering structures.*

Key Words: Peridynamics, Bond-based theory, Crack growth, Brittle material, Failure.

1. INTRODUCTION

Finite element method (FEM) is widely used in various applications in solid mechanics [1-7]. However, the FEM equations become singular in presence of discontinuities such as cracks. Therefore, additional efforts are required to make the FEM sufficient in fracture mechanics. Extended finite elements (XFEM) and cohesive zone model (CZM) are improvements on the classical FEM to avoid singularity around the crack tip. CZM [8, 9] is mesh dependent, where crack can only follow between the elements. Although XFEM [10, 11] can predict arbitrary crack growth, it is computationally costly. Furthermore, both methods require an extra criterion to obtain the crack growth path.

Since most of the FE methods are costly, there is always a need to more efficient methods. Spectral finite element is a computationally very efficient alternative. The drawback of the spectral finite element is in modelling complex and realistic structures. Khalili et al. [12-14] formulated WSFE-based elements and implemented them in Abaqus through user defined element (UEL) subroutine. The WSFE-based UEL has the computational efficiency of the WSFE and also is capable of modelling realistic structures. The WSFE-based UEL is a huge step forward since the introduction of spectral finite element to the FEM. Later one they even proved the ability of the WSFE-based UEL in generating baseline data for structural health monitoring (SHM) purposes [15].

Peridynamics is an alternative continuum mechanic formulation which reformulates the equation of motion by substituting differential terms with integral terms [16-23]. Therefore, the peridynamic equations are valid in discontinuities and consequently is a perfect technique in predicting material failure. Furthermore, the damage modeling is an inherent feature of the peridynamics and there is no need for extra criteria for crack initiations and propagation. Ha and Bobaru [24] studied dynamic crack branching in brittle materials using peridynamics. Yaghoobi and Chorzepa [25] used peridynamics to predict the response of fiber reinforced concrete (FRC) structures.

Chorzepa and Yaghoobi [26] used peridynamics to investigate fracture in FRC beams under dynamic loading. A mesoscale modeling of cementitious composites are conducted by Yaghoobi et al. [27] to investigate damage mechanics using peridynamics.

The main focus of this work is to study the ability of peridynamics to accurately predict the complex failure modes of a material. In doing so, a 2D peridynamic model is provided. In addition to a symmetric macro crack, asymmetric circular notches are provided in the plate. The number of the circular notches and their positions are varying in different simulations to study if peridynamics is able to predict unguided and complex crack growth. The original peridynamic form, so called “bond-based peridynamics”, is used in this study. Despite of some limitations such as a fixed Poisson’s ratio [17,21], BBPD has been proven very robust technique is fracture mechanics. The material is assumed to be linear elastic and fracture is occurred with no plastic deformation. Results indicate that the presented modeling method provides a promising technique in fracture analysis of asymmetric bodies.

2. THEORY

The classical continuum theory is based on the assumption that material points interact only with their nearest neighboring points. In the peridynamic theory, a material point is influenced by any points within a finite distance as shown in Fig. 1. Peridynamic equation of motion of a material point at $\mathbf{x}$ and time t in the reference configuration is written as [17]

$$\rho\ddot{\mathbf{u}}(\mathbf{x},t) = \int_{H_{\mathbf{x}}} \mathbf{f}(\mathbf{x},\mathbf{x}',\mathbf{u}(\mathbf{x},t),\mathbf{u}(\mathbf{x}',t))\, dV_{\mathbf{x}'} + \mathbf{b}(\mathbf{x},t)$$
(1)

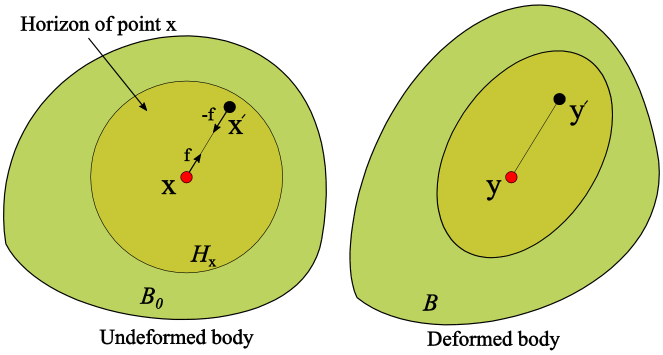

Fig -1 Schematic representation of peridynamic body.

where $\mathbf{u}$ is the displacement vector field, ρ is the mass density and $\mathbf{b}(\mathbf{x},t)$ is the body force acting at $\mathbf{x}$ at time t. $\mathbf{f}$ is the pairwise force function, also known as the peridynamic bond that connects point $\mathbf{x}'$ to $\mathbf{x}$.

Note that the integral is defined over a region $H_{\mathbf{x}}$, which in two dimension is taken to be a circle of radius δ called the "horizon". Also the relative position of these two points in the reference configuration is given by

$$\boldsymbol{\xi} = \mathbf{x}' - \mathbf{x}$$
(2)

and their relative displacement by

$$\boldsymbol{\eta} = \mathbf{u}(\mathbf{x}',t) - \mathbf{u}(\mathbf{x},t) \quad (3)$$

It is worth mentioning that $\mathbf{y}' - \mathbf{y} = \boldsymbol{\xi} + \boldsymbol{\eta}$ represents the current relative position vector connecting the particles. A micro-elastic material is defined as one for which the pairwise force derives from a micro-potential, ω [17]

$$\mathbf{f}(\boldsymbol{\eta},\boldsymbol{\xi}) = \frac{\partial\omega(\boldsymbol{\eta},\boldsymbol{\xi})}{\partial\boldsymbol{\eta}}$$
(4)

The strain energy density at a given point is

$$W(\mathbf{x}) = \frac{1}{2}\int_{H_{\mathbf{x}}} \omega(\boldsymbol{\eta},\boldsymbol{\xi})\, dV_{\mathbf{x}'}$$
(5)

The factor of a half in Eq. (5) is present because the elastic energy in a bond is shared by the two points connected by the bond. A micro-elastic potential, which leads to a linear relationship between the bond force and the relative elongation of the bond, is obtained if we take

$$\omega(\boldsymbol{\eta},\boldsymbol{\xi}) = \frac{1}{2}cs^2$$
(6)

where c, called ``micromodulus", is a material parameter and s is the bond relative elongation.

$$s = \frac{|\boldsymbol{\xi}+\boldsymbol{\eta}|-|\boldsymbol{\xi}|}{|\boldsymbol{\xi}|}$$
(7)

Note that $|\mathbf{A}|$ represents the length of a vector $\mathbf{A}$. The corresponding pairwise force becomes

$$\mathbf{f}(\boldsymbol{\eta},\boldsymbol{\xi}) = \frac{\partial\omega(\boldsymbol{\eta},\boldsymbol{\xi})}{\partial\boldsymbol{\eta}} = cs\,\frac{\boldsymbol{\xi}+\boldsymbol{\eta}}{|\boldsymbol{\xi}+\boldsymbol{\eta}|}$$
(8)

$\frac{\boldsymbol{\xi}+\boldsymbol{\eta}}{|\boldsymbol{\xi}+\boldsymbol{\eta}|}$ is the unit vector along the direction of vector $\boldsymbol{\xi}+\boldsymbol{\eta}$, the bond between $\mathbf{x}$ and $\mathbf{x}'$ in the deformed configuration. The value of the micromodulus corresponding to a given bulk modulus B, and for isotropic materials, is computed by matching the peridynamic strain energy density to the classical strain energy density [17].

$$c = \frac{18B}{\pi\delta^4}$$
(9)

Note that if the stretch between two points reaches to its critical stretch, s_0, the bond is broken. To model bond breakage, a weight function is defined as

$$\mu(\boldsymbol{\eta},\boldsymbol{\xi}) = \begin{cases} 1 & \text{if } s < s_0 \\ 0 & \text{otherwise} \end{cases}$$
(10)

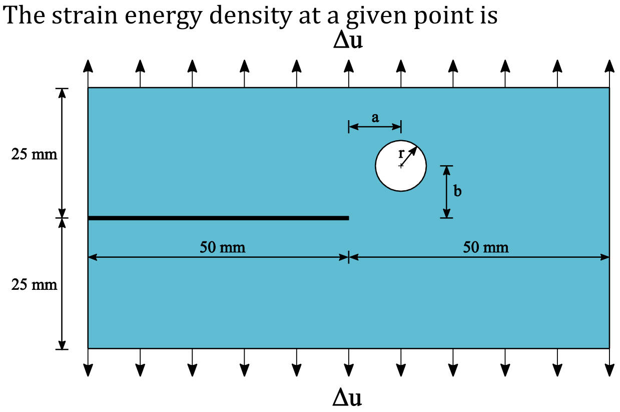

(a) Model I

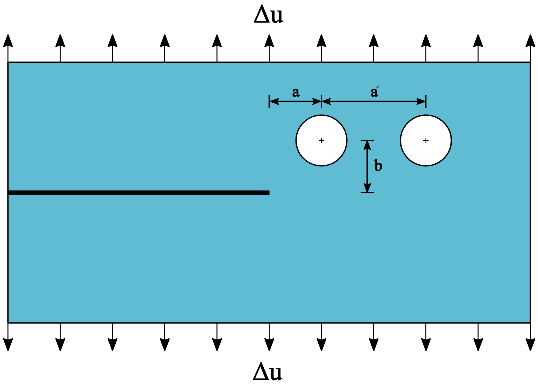

(b) Model II

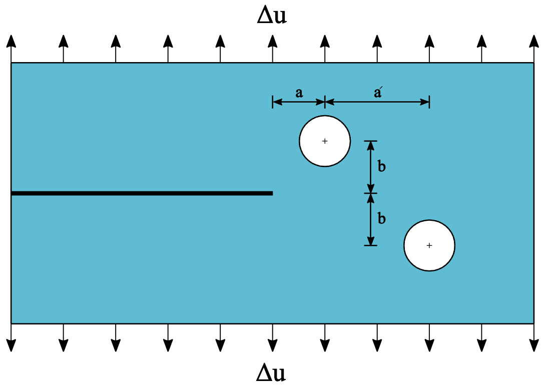

(c) Model III

Fig -2 Schematic of the pre-cracked model with asymmetric circular notches subjected to tension.

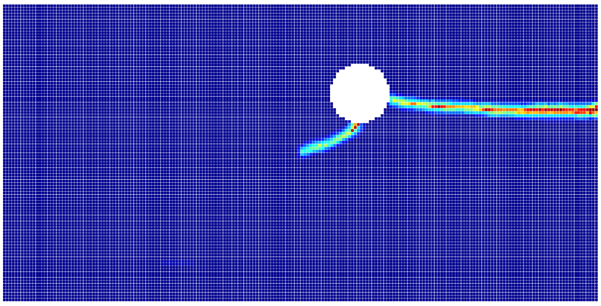

(a) $a = 10\,mm$

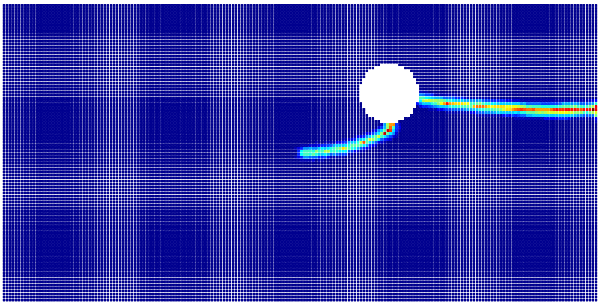

(b) $a = 15\,mm$

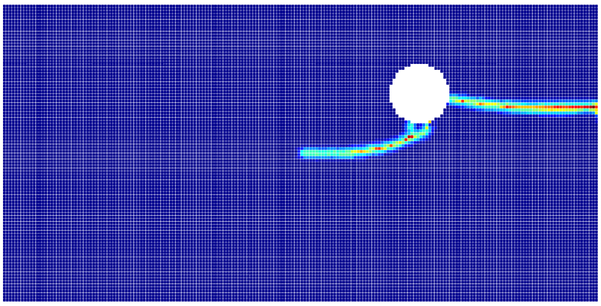

(c) $a = 20\,mm$

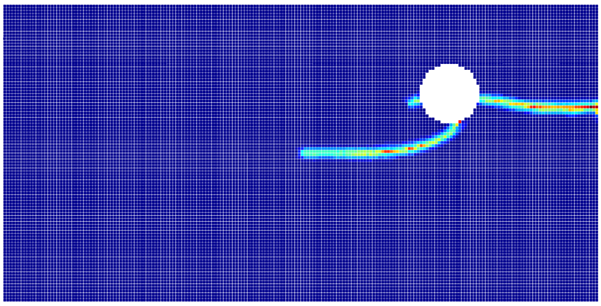

(d) $a = 25\,mm$

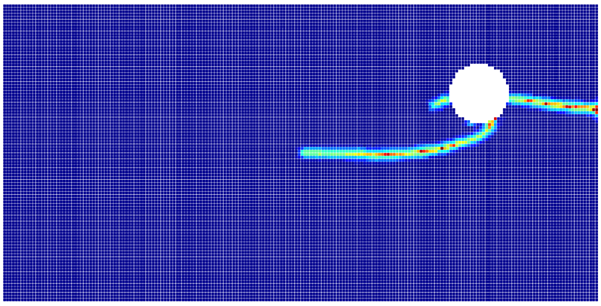

(e) $a = 30\,mm$

Fig -3 Crack pattern for five cases of Model I with $b = 10\,mm$ and varying a.

Therefore, the pairwise force in Eq. (8) is updated to take into account the bond breakage as follows

$$\mathbf{f}(\boldsymbol{\eta},\boldsymbol{\xi}) = \mu(\boldsymbol{\eta},\boldsymbol{\xi}) cs \frac{\boldsymbol{\xi}+\boldsymbol{\eta}}{|\boldsymbol{\xi}+\boldsymbol{\eta}|}$$

(11)

For the peridynamic point $\mathbf{x}$, a damage factor is defined as follows

$$\varphi(\mathbf{x},t) = 1 - \frac{\int_{H_{\mathbf{x}}} \mu(\boldsymbol{\eta},\boldsymbol{\xi})\, dV_{\mathbf{x}'}}{\int_{H_{\mathbf{x}}} dV_{\mathbf{x}'}}$$

(12)

The damage factor resembles the ratio of broken bonds over total number of bong initially connected to point **x.**

Note that, $0 \le \varphi \le 1$, with 0 representing no damaged material, and 1 representing complete disconnection of the point from all of the points with which it initially interacted. In Section 4, φ is used is illustrating plot damage evaluations.

3. ANALYTICAL MODEL

A two-dimensional $100\ mm\ \times 50\ mm$ plannar model is developed. As seen in Fig. 2, the symmetric macro crack with length of $50\ mm$ is provided in the model. Furthermore, asymmetric circular notches with radius of $r = 5\ mm$ are provided in order to study the unguided crack growth. Three main sets of models are provided based on the number and arrangement of circular notches. The first set, indicated as "Model I" in Fig. 2a has a single notch. For this case, five different cases are provided by varying the notch location. The second and the third sets have two circular notches, but with different arrangement (see Fig. 2b,c). Varying the horizontal location of the second notch, hereinafter referred to as the "right notch", five different cases are designed for each model.

A linear elastic material is assumed with brittle fracture. Therefore, no plastic deformation is occurred during damage process. Mechanical properties is provided in Table 1. The quadrilateral peridynamic point distribution is utilized with point spacing (grid size) of $h = 0.5\ mm$. The horizon size is selected as $\delta = 3h$. The critical stretch is taken as $s_0 = f_t/E$.

As seen in Fig. 2, displacement loading, $\Delta u = 0.002\ mm$, is applied to both side of the plate. Therefore, the beam is subjected to total displacement loading of $2\Delta u = 0.004\ mm$. The displacement loading is applied in a quasi-static state. Under the quasi-static loading condition, the equilibrium system of equations is obtained by eliminating acceleration term in Eq. (1).

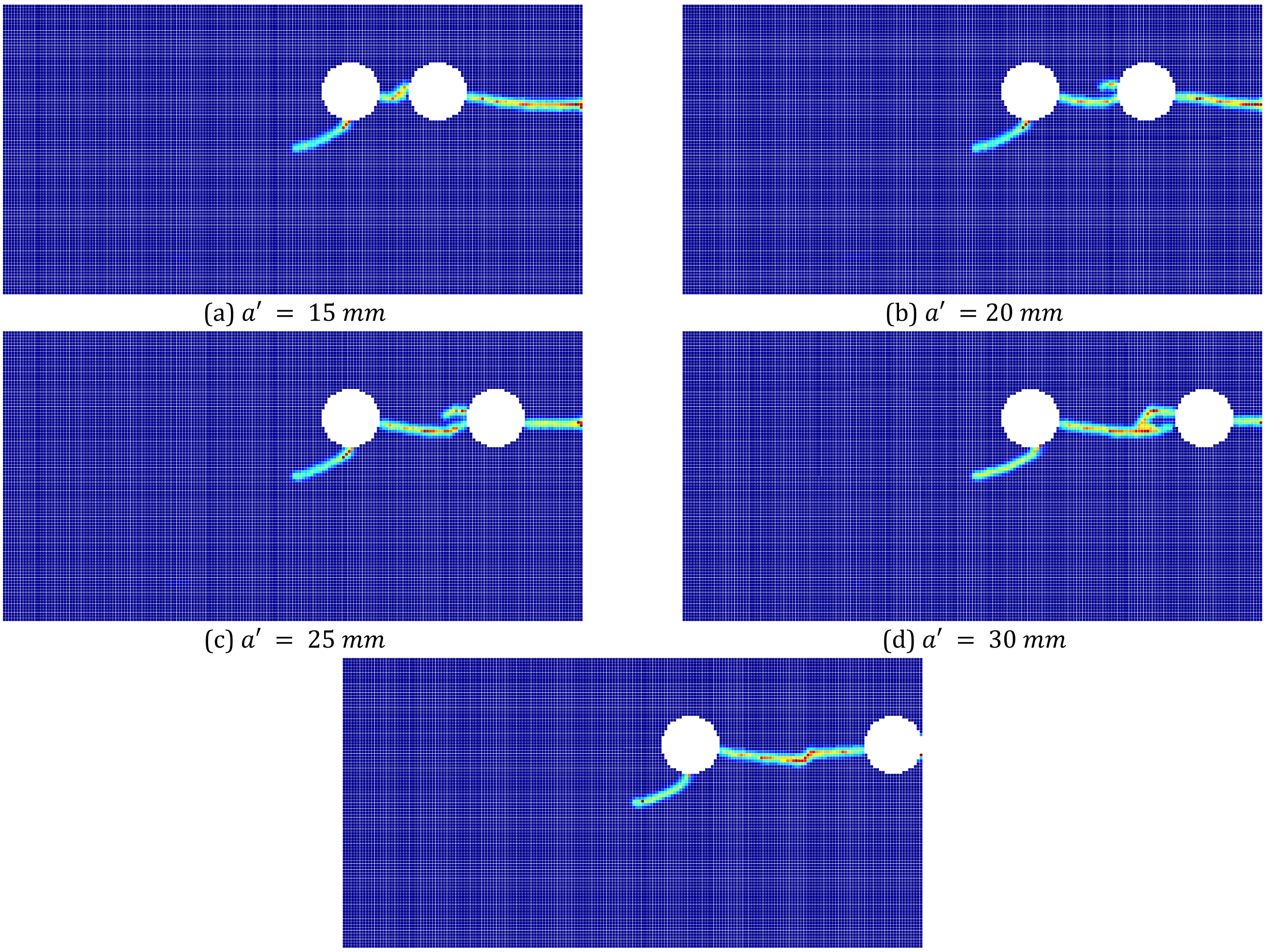

(a) $a' = 15\ mm$ (b) $a' = 20\ mm$ (c) $a' = 25\ mm$ (d) $a' = 30\ mm$ (e) $a' = 35\ mm$

Fig -4 Crack pattern for five cases of Model II with $a = 10\ mm$, $b = 10\ mm$ and varying a'.

An incremental-iterative method is employed to obtain the equilibrium system. Dynamic relaxation method [28] is adopted in order to solve the peridynamic system of equations. The application of dynamic relation method in peridynamics are explained by Kilic and Madenci [29] and Yaghoobi and Chorzepa [25]. The sensitivity of results to mesh size was inspected as well [30, 31]. Crack growth and development caused by external tension have been studied in case of a composite [32] or metallic samples [33, 34].

Table -1: Mechanical properties of the plate material.

Elastic Modulus, $E(MPa)$	Poisson's ratio, υ	Tensile strength, f_t (MPa)
20,000	0.25	2

4. RESULTS

Figs. 3-5 illustrate the predicted crack growth patterns using the bond-based peridynamics. In these figures, crack is represented using the peridynamic point damage factor, φ, defined in Eq. (12). Blue color represents points with no damage, $\varphi = 0$, and red color illustrates points with complete disconnection from all of the points, $\varphi = 1$.

Fig. 3 shows the results for cases belong to Model I (see Fig. 2a). Five different cases are analysed for varying the position of the circular notch. In all cases, the macro crack grows from the crack tip and ends to the circular notch in a curve-shaped path. Then, another crack is initiated and grows from the notch to the specimen's wall. By positioning the notch far away from the crack tip (see Figs. 3d and 3e) a third crack is observed initiated from the notch growing to the left side.

Fig. 4 illustrates the damage pattern for cases belong to Model II (see Fig. 2b). Five different cases are studied with fixed position of the left notch, while the right notch position is varying. In all cases the macro crack grows from the crack tip to the left notch. Then, it continues to grow from the notch to the right notch. Meanwhile, a smaller and parallel crack is initiated from the right notch approaching to the left notch. When two notches are relatively close (see Figs. 4a-c), the larger crack initiating from the left notch reaches to the right notch. In other cases (see Figs. 4d-e), the cracks between two notches are coalesced. In all cases, the final fracture stage is a crack initiating from the right notch approaching to the specimen's wall.

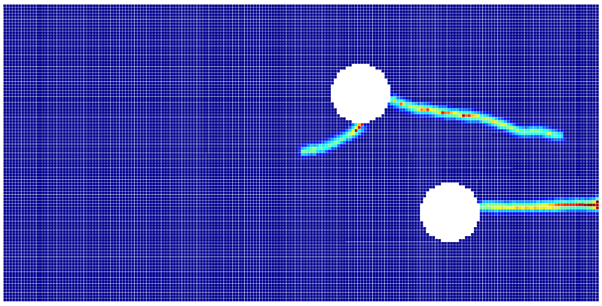

(a) $a' = 15\ mm$

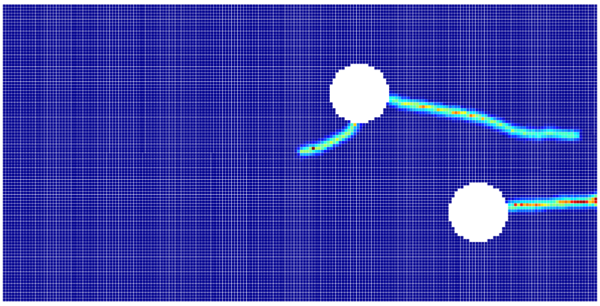

(b) $a' = 20\ mm$

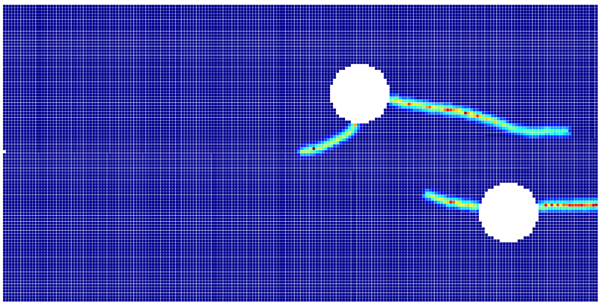

(c) $a' = 25\ mm$

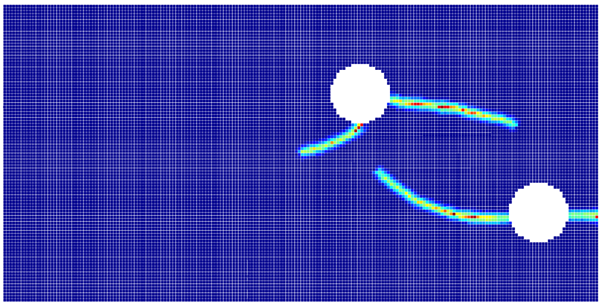

(d) $a' = 30\ mm$

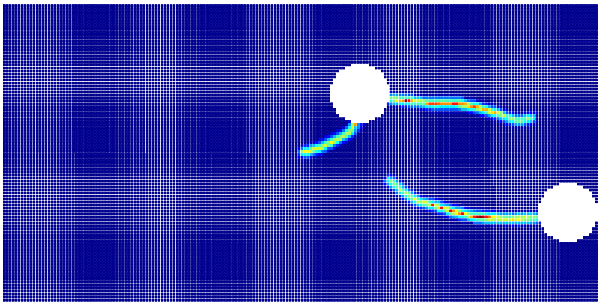

(e) $a' = 35\ mm$

Fig -5 Crack pattern for five cases of Model III with $a = 10\ mm, b = 10\ mm$ and varying a'.

The damage pattern for the cases belong to the Model III are presented in Fig. 5. Five cases are provided where the position of the top notch is fixed with varying position of the bottom notch. Similar to the cases of Model I, the major damage in these cases is the growth of macro crack to the top notch followed by a crack initiated from the top notch approaching to the specimen's wall.

Furthermore, damage is also observed around the bottom notch. For cases in which the bottom notch is far away the specimen notch, a single crack is initiated and grows to the specimen's wall (see Figs. 5a,b). When the bottom notch is near the specimen notch, a curve-shaped crack is initiated from the bottom notch growing to the top notch (see Figs. 5c-e).

5. CONCLUSION

This paper employs peridynamics in order to study the effect of asymmetric circular notches on fracture behaviour of pre-cracked specimens. The following conclusions can be drawn from above works:

- Peridynamics is a promising technique in modelling discontinuities such as cracks.
- Peridynamics only require a single bond breakage criteria.
- There is no need for extra criterion for crack initiation, propagation, coalescence and to obtain crack growth path. In other word, peridynamics unifies the damage prediction requirements.
- Peridynamics can successfully predict the unguided crack growth in asymmetric specimens.

While the present work builds a distinct framework for fracture analysis of asymmetric specimens and structures, future works includes:

- Study of refinement in peridynamic point spacing and to study the effect of horizon size on crack growth pattern.
- Enhancing material model to cover nonlinear behaviour.
- Extending the presented approach to three-dimensional models.

REFERENCES

[1] Zienkiewicz, Olek C., and Robert L. Taylor. The finite element method for solid and structural mechanics. Butterworth-heinemann, 2005.

[2] Hughes, Thomas JR. The finite element method: linear static and dynamic finite element analysis. Courier Corporation, 2012.

[3] Chakherlou, T.N. and Yaghoobi A. "Numerical simulation of residual stress relaxation around a cold-expanded fastener hole under longitudinal cyclic loading using different kinematic hardening models." Fatigue & Fracture of Engineering Materials & Structures 33.11 (2010): 740-751.

[4] Jafari-Shiadeh, S.M., Ardebili, M. and Moamaei, P. "Three-dimensional finite-element-model investigation of axial-flux PM BLDC machines with similar pole and slot combination for electric vehicles", In: Proceedings of Power and Energy Conference, Illinois, pp. 1–4, 2015

[5] Jafari-Shiadeh, S.M. and Ardebili, M. "Analysis and comparison of axial-flux permanent-magnet brushless-DC machines with fractional-slot concentrated-windings", Proc. 4th Annu. Int. Power Electron., Drive Syst., Technol. Conf., pp. 72-77, 2013.

[6] Yaghoobi, A. "Implementation of nonlinear finite element Using object–oriented design patterns." Journal of Mechanical Engineering and Technology (JMET) 4.1 (2012).

[7] Yaghoobi, A. (2009) Finite Element Analysis of Pressure Vessels and Fastener Holes in Elastic-Plastic Region using Radial Return Algorithm. Msc Thesis, University of Tabriz, Tabriz, Iran.

[8] Elices, M.G.G.V., Guinea, G.V., Gomez, J. and Planas, J. "The cohesive zone model: advantages, limitations and challenges." Engineering fracture mechanics 69.2 (2002): 137-163.

[9] Xie, D. and Waas, A.M. "Discrete cohesive zone model for mixed-mode fracture using finite element analysis." Engineering fracture mechanics 73.13 (2006): 1783-1796.

[10] Fries, T.P. and Belytschko, T. "The extended/generalized finite element method: an overview of the method and its applications." International Journal for Numerical Methods in Engineering 84.3 (2010): 253-304.

[11] Fries, T.P., Zilian, A. and Moës, N. "Extended Finite Element Method." International Journal for Numerical Methods in Engineering 86.4-5 (2011): 403-403.

[12] Khalili A., Jha R., Samaratunga D. "The Wavelet Spectral Finite Element-Based User-Defined Element in Abaqus for Wave Propagation in One-Dimensional Composite Structures" Simulation: Transactions of the Society for Modeling and Simulation International, January 23, 2017, DOI: 10.1177/0037549716687377

[13] Khalili A., Jha R., Samaratunga D. "Spectrally Formulated User-Defined Element in Conventional Finite Element Environment for Wave Motion Analysis in 2-D Composite Structures" European Journal of Computational Mechanics, 25 (6), 2016, pp. 446-474, DOI: 10.1080/17797179.2016.1253364

[14] Khalili A., Samaratunga D., Jha R., Lacy T. E., Gopalakrishnan S. "WSFE-based User-Defined Elements in ABAQUS for Modeling 2D Laminated Composites with Complex Features" 30th ASC Technical Conference, Michigan State University, East Lansing, MI, US, 28-30 September 2015.

[15] Khalili A., Jayakody N., Jha R. "Structural Health Monitoring of Skin-Stiffener Composite Structures Using WSFE-based User Defined Elements in Abaqus" 25th AIAA/AHS Adaptive Structures Conference, Grapevine, TX, US, 9-13 January 2017. DOI: 10.2514/6.2017-1677

[16] Silling, S.A. "Reformulation of elasticity theory for discontinuities and long-range forces." Journal of the Mechanics and Physics of Solids 48.1 (2000): 175-209.

[17] Silling, S.A. and Askari, E. "A meshfree method based on the peridynamic model of solid mechanics." Computers & structures 83.17 (2005): 1526-1535.

[18] Silling S.A., Epton M., Weckner O., Xu J. and Askari E. " Peridynamic states and constitutive modeling." Journal of Elasticity 88.2 (2007): 151-184.

[19] Warren, T. L., Silling, S.A., Askari, A., Weckner, O., Epton, M. A. and Xu, J. "A non-ordinary state-based peridynamic method to model solid material

deformation and fracture." International Journal of Solids and Structures 46.5 (2009): 1186-1195.

[20] Breitenfeld, M.S., Geubelle, P.H., Weckner, O. and Silling, S.A. (2014). Non-ordinary state-based peridynamic analysis of stationary crack problems. Computer Methods in Applied Mechanics and Engineering, 272, 233-250.

[21] Yaghoobi, A. and Chorzepa, M. G. "Fracture analysis of fiber reinforced concrete structures in the micropolar peridynamic analysis framework." Engineering Fracture Mechanics 169 (2017): 238-250.

[22] Yaghoobi, A. and Chorzepa, M. G. "Formulation of symmetry boundary modeling in non-ordinary state-based peridynamics and coupling with FEA." Mathematics and Mechanics of Solids (2017).

[23] Yaghoobi, A. and Chorzepa, M.G. "Higher-order approximation to suppress the zero-energy mode in non-ordinary state-based peridynamics." Computers & Structures (2017).

[24] Ha, Y.D. and Bobaru, F. "Studies of dynamic crack propagation and crack branching with peridynamics." International Journal of Fracture 162.1-2 (2010): 229-244.

[25] Yaghoobi, A. and Chorzepa, M. G. "Meshless modeling framework for fiber reinforced concrete structures." Computers & Structures 161 (2015): 43-54.

[26] Chorzepa, M.G. and Yaghoobi, A. "Innovative Meshless Computational Method for the Analysis of Fiber-Reinforced Concrete (FRC) Structures." Geotechnical and Structural Engineering Congress 2016.

[27] Yaghoobi, A., Chorzepa, M.G., Kim, S.S. and Durham, S.A. Mesoscale fracture analysis of multiphase cementitious composites using peridynamics. Materials 2017, 10 (2), 162; doi:10.3390/ma10020162.

[28] Zhang, L.G. and Yu, T.X. "Modified adaptive dynamic relaxation method and its application to elastic-plastic bending and wrinkling of circular plates." Computers & structures 33.2 (1989): 609-614.

[29] Kilic, B. and Madenci E. "An adaptive dynamic relaxation method for quasi-static simulations using the peridynamic theory." Theoretical and Applied Fracture Mechanics 53.3 (2010): 194-204.

[30] M. Masoomi, S. M. Thompson, N. Shamsaei, A. Elwany, and L. Bian, "An experimental-numerical investigation of heat transfer during selective laser melting," in 26th International Solid Freeform Fabrication Symposium, 2015.

[31] M. Masoomi, N. Shamsaei, X. Gao, S. M. Thompson, A. Elwany, L. Bian, N. Shamsaei, L. Bian, and A. Elwany, "Modeling, simulation and experimental validation of heat transfer during selective laser melting," in ASME 2015 International Mechanical Engineering Congress & Exposition, 2015.

[32] P. Gharghabi, J. Lee, M. S. Mazzola and T. E. Lacy, "Development of an Experimental Setup to Analyze Carbon/Epoxy Composite Subjected to Current Impulses," in Proceedings of the American Society for Composites: Thirty-First Technical Conference, VA, 2016.

[33] P. Gharghabi, P. Dordizadeh B., and K. Niayesh, "Impact of Metal Thickness and Field-Shaper on the Time-Variant Processes during Impulse Electromagnetic Forming in Tubular Geometries," Journal of the Korean Physical Society, vol. 59, no. 6, p. 3560, 2011. doi.org/10.3938/jkps.59.3560

[34] P. Dordizadeh-Basirabad, P. Gharghabi, and K. Niayesh, "Dynamic Analysis of a Fast-acting Circuit Breaker (Thompson) Drive Mechanism," Journal of the Korean Physical Society. vol. 59, no. 6, p. 3547, 2011. doi.org/10.3938/jkps.59.3547